SIMULATION STUDIES OF ADVANCED INFRARED AND MICROWAVE SOUNDERS

Christopher D. Barnet
General Sciences Corporation, a subsidiary of Science Applications International Corporation
Beltsville, Maryland, USA

Joel Susskind
NASA Goddard Space Flight Center
Greenbelt, Maryland, USA

1 Abstract

We will discuss simulation studies which assess the relative performance of advanced multi-spectral (infrared and microwave) sounders with regard to meeting environmental sounding requirements of the National Aeronautics and Space Administration (NASA) and the National Polar-orbiting Operational Environmental Satellite System (NPOESS).

These studies used advanced retrieval techniques to capture the information content of high resolving power instruments. We include a brief overview of salient features of the retrieval algorithm. Results include soundings of temperature, moisture, and ozone within partially cloudy conditions (50 km footprints with up to 80 % cloudiness) for the NASA/AIRS, the notional European meteorological satellites (EUMETSAT) IASI, and the notional NPOESS/CrIS instruments. Trade studies involving spectral resolution and signal-to-noise will also be shown.

2 Introduction

We performed a simulation study to evaluate future advanced Earth sounding instruments. Figure 1 shows the spectral coverage of the instruments considered in this study. The Atmospheric Infrared Sounder (AIRS) instrument (*Aumann* 1994) has 2378 discrete channels covering 17 spectral bands. Each band has a sampling at $\approx \frac{\nu}{2400}$ cm^{-1}, where ν is wavenumber in cm^{-1}. The notional Infrared Atmospheric Sounding Interferometer (IASI) instrument (*Cayla* 1993) has three spectral bands which provide continuous spectral coverage from 645 cm^{-1} to 2760 cm^{-1} with a spectral sampling of

Table 1: Summary of Instrument Characteristics

parameter	AIRS	IASI	NPOESS notional CrIS
# channels	2378	9230	1400
L, Optical Path Difference	n/a	2 cm	0.8/0.4/0.2 cm
Spectral Sampling	$\approx \nu/2400$ cm^{-1}	0.25 cm^{-1}	0.625/1.25/2.5 cm^{-1}
Unapodized FWHM	n/a	0.302 cm^{-1}	0.754,1.51, 3.02
# IR FOVs per AMSU-A FOV	9	4	9
A, Effective Aperture (cm)	n/a	8	4
Ω, IFOV	1.1°	0.825°	0.825°
Altitude (km)	705	833	833
projected IFOV Size (km)	13.5	12	12
Apodization Function	$\approx$ Gaussian	Gaussian	Hamming
$\Delta\nu$, Apodized Resolution (FWHM)	$\approx \nu/1200$ cm^{-1}	0.5 cm^{-1}	1.125/2.25/4.5 cm^{-1}
Noise Reduction Factor, f	n/a	1.7	1.58
Noise Correlation (%) with adjacent channels	n/a	71,25,4.4,...	68,13

0.25 cm^{-1}. The NPOESS Cross-track Interferometric Sounder (CrIS) instrument (*IPO* 1998) is not specified at this time; however, the notional instrument has three spectral bands covering 635-1095 cm^{-1}, 1210-1540 cm^{-1}, and 2155-2450 cm^{-1} with a sampling of 0.625, 1.25, and 2.5 cm^{-1} respectively. These characteristics are summarized in Table 1. We have chosen to use apodized radiances for the interferometers and will discuss this in the AIRS/NPOESS retrieval algorithm section. Notice in Table 1 that the AIRS and IASI have comparable spectral resolution in the long-wave temperature sounding region (i.e., $\approx$ 700 cm^{-1}) and that the notional CrIS instrument has significantly less spectral resolution and spectral sampling in this region. AIRS and IASI have the same spectral sampling in the long-wave; however, the noise in adjacent channels of the apodized IASI is strongly correlated.

The IASI simulations in this study are preliminary. Two simplifications were made for IASI to provide these simulations is a timely manner:

- This simulation dataset was not designed to simulate cloud contrast as a function of field of view (FOV). Improvement in the cloudy simulation may occur if IASI's notional 9-km footprint improves cloud contrast compared to the somewhat larger footprints of the other instruments. The IASI radiance simulation computes nine 1.1° (15-km) footprints per AMSU 3.3° footprint, rather than the four smaller footprints currently proposed for IASI. We select the four footprints with the highest radiance contrast in the 8 μm region. Therefore, we have given IASI the highest possible cloud contrast (smallest cloud clearing extrapolation from clearest spot) in the retrieval. We believe this over compensates for any cloud contrast enhancements due to the smaller FOV.

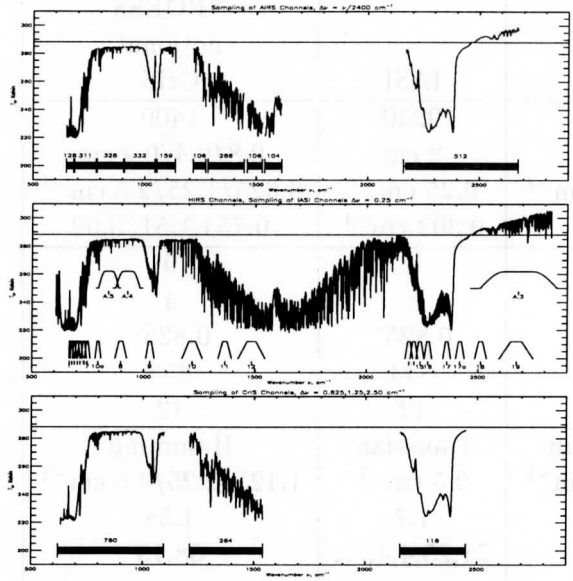

Figure 1: Illustration of the spectral coverage of AIRS (top panel), IASI (middle panel), and the notional NPOESS CrIS instrument (bottom panel). The HIRS channels are shown in the middle panel along with AVHRR channels 3, 4, and 5.

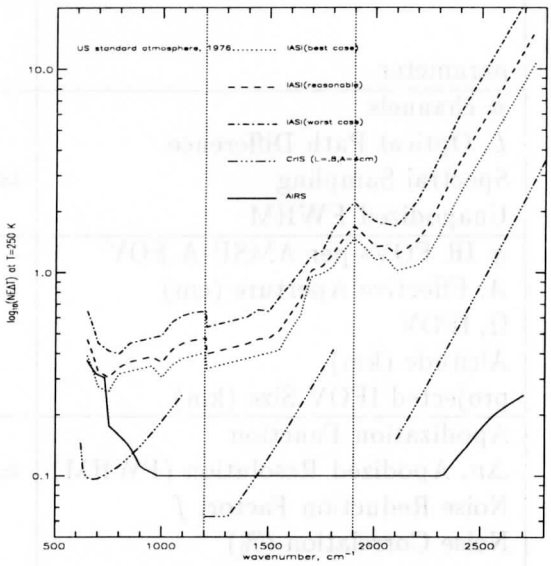

Figure 2: Noise models used within the simulation. All noise models have been converted to NEΔT, evaluated at 250° K, per spectral sample. All noise estimates are for the apodization function shown in Table 1 and include the apodized noise reduction factor. Apodized noise is correlated with neighboring channels (see text).

- IASI's first guess is an AIRS regression retrieval, using the same 4 FOV's as IASI. Future versions will include an IASI regression first guess using all IASI channels. The effect on the retrieval results could either improve (due to the increase spectral resolution and coverage of IASI at shorter wavelengths) or degrade (due to the larger instrumental noise of IASI).

We assume that the observing platform has a co-located microwave measurement capability similar to AMSU-A and AMSU-B. AMSU-B is functionally equivalent to the microwave humidity sounder (MHS) and the humidity sounder Brazil (HSB).

3 Instrumental rapid transmittance algorithms and noise models

The University of Maryland Baltimore County (UMBC) (*Hannon* 1996) developed, for use by the AIRS and IASI Science Teams and the NPOESS CrIS community, the rapid transmittance algorithms (RTA) for all three instruments in this study. The RTA's produce apodized channel averaged transmittances for use in channel averaged radiative transfer computations. The vertical pressure grid is 100 layers spaced logarithmically from a pressure of 0.005 mb to 1100 mb.

The AIRS channel response function model used in the RTA and noise estimates are from preliminary design review (PDR) engineering studies. We used a minimum noise value of 0.1° K in an effort to account for other noise sources. We expect no significant correlation of AIRS noise with neighboring channels. Fig. 2 shows the AIRS noise estimate a solid line. Recent flight model measurements of the AIRS instrument PM-1 channel spectral response function and channel noise indicate a superior version to the models used here.

The IASI noise model is taken from a noise estimate distributed electronically by F. Cayla in Dec. 1997. Three noise models were given: best, reasonable, and worst case. The noise for all three cases uses a a Gaussian apodized spectrum and includes noise estimates due to spectral calibration error, channel response function error, and other pseudo-noise sources. The three apodized IASI models are shown in Fig. 2 as dotted, dashed, and dash-dotted lines respectively. IASI's Gaussian apodization has a statistical noise reduction factor of $f_G \simeq 1.7$. In the simulation of radiances, an uncorrelated noise spectrum (normal distribution with $\sigma = f_G \cdot \mathrm{NE}\Delta\mathrm{N}$) is computed and then apodized with IASI's Gaussian apodization function. The apodized noise spectrum, correlated with adjacent channels, is then added to the radiances. The retrievals noise covariance matrix uses a statistical estimate of the noise correlation factors with neighboring channels with values shown in Table 1.

The notional CrIS RTA uses a Hamming apodization. This apodization function is less severe than IASI's Gaussian apodization and, therefore, has a lower statistical noise reduction factor of f_H=1.58. The radiances are simulated in the same manner as the IASI instrument. The retrievals noise covariance matrices use a statistical channel noise correlation of a Hamming function shown in Table 1. Lincoln Laboratories developed the notional for the Integrated Programs Office (IPO). It assumes that the clear aperture of the interferometer is 4 cm and uses optimistic estimates for optical and detector parameters.

The region near 665 cm^{-1} is useful for the stratospheric temperature sounding. Every available channel is used in this region. The IASI instrument has comparable noise to the AIRS instrument; however, the noise is correlated among adjacent channels. Thus, IASI has a higher effective noise (less noise reduction when spectral averaging) than the AIRS and, therefore, is expected to degrade slightly. The CrIS instrument has lower noise in this region; however there are significantly fewer channels available and the noise is also correlated.

Note, optimization for lower noise can occur for both IASI and CrIS. Using an $L = 1$ cm "sounding mode" for IASI would improve the noise the noise at the expense of spectral resolution and sampling. CrIS could be designed to integrate for the full 160 ms in Band #2 and #3.

The spectral region $670 < \nu < 720$ cm^{-1} is critical for the upper tropospheric temperature sounding.

Table 2: Summary of AIRS Science Team Scan Lines used for testing. % cloud refers to the % cloud fraction of a AMSU footprint

test ID#	scan ID#	D/N	range % clouds	lat.	long.	$< T_s >$ range	Location
1, 2	25, 26	D	1-53	11	80	300	Indian Ocean/India
3, 4	87, 88	D	0-93	40	63	275-290	Kazakh (former USSR)
5, 6	171,171	N	46-96	77	25	266-277	north polar
7, 8	311,312	N	31-69	28	-110	291-295	Baja California, Mexico
9,10	370,371	N	2-41	0	-116	295-297	Eastern Pacific
11,12	453,454	N	68-90	-38	-128	284-287	S.E. Pacific
13,14	539,540	D	3-91	-75	-160	249-257	Antarctica
15,16	633,634	D	5-82	-51	65	274-277	S.Indian Ocean

In this region, AIRS and IASI have similar sampling, resolution, and noise. IASI's correlated noise design continues to play a role in this region since channels in the wings of lines are effectively averaged to increase signal-to-noise. The CrIS instrument has significantly less sampling and poorer spectral resolution; however, the notional noise estimate is very low in this wavelength region.

The spectral region $720 < \nu < 750$ cm^{-1} is useful for mid- to lower tropospheric temperatures sounding. In this region, CrIS and AIRS have good noise characteristics. The shortwave region near 2380 cm^{-1} is most important for lower tropospheric temperature sounding. Spectral resolution does not play a role here as none of the instruments resolve any spectral features. AIRS has a significantly lower noise than CrIS or IASI, however.

4 The AIRS Science Team's Simulation Dataset

AIRS derived its orbital simulation from a global simulation using a version of the operational general circulation model (GCM) from NOAA NCEP for Nov. 5, 1996 (8:30 to 10:00 UT). The fields in the GCM are 2.5 degree by 2.5 degree gridded data from a spectral model of NCEP (*Juang* 1997). The temperature, ozone and the liquid water are at 29 levels from 1015 mb to 3 mb. The water vapor profiles are at 12 levels from 1015 to 300 mb.

The dependent data set (from now on called the "training dataset") is 149 AMSU scan lines (each containing 30 AMSU-A footprints) selected from every fifth scanline from a full simulated orbit on Nov. 6, 1996. The independent dataset (from now on called the "truth") is 8 pairs of individual AMSU scan lines (30 AMSU-A footprints, 270 MHS footprints, 270 AIRS footprints per AMSU scan line) from a 6 hour GCM forecast with characteristics shown in Table 2. A first guess of all the geophysical parameters (including surface pressure) taken from an 18 hour GCM forecast is available for use in the retrieval.

Computation of the forecast fields at the given location for the two time periods from the four surrounding points uses a bi-linear interpolation method. To get the data at the given time a time interpolation of the forecast data is performed. Generation of fields in the vertical layers necessary for the AIRS retrieval software required performing a vertical interpolation of forecast fields. Every field varies spatially, to some extent, within the AMSU footprint.

Note that this linear interpolation of 2.5 degree by 2.5 degree gridded data produces smooth fields; however, the cloud clearing algorithm depends on the contrasts between AIRS/MHS footprints within an AMSU footprint. Therefore, the cloud fraction, cloud emissivity, cloud top pressure, and cloud reflectivity were randomized at the end of the interpolation process. The artificially smooth fields, especially water vapor fields and surface parameters, will be studied and improved upon later, if necessary.

The top of the forecast model data is at 300 mb for water vapor profile and 3 mb for others. The water vapor is extrapolated above 300 mb by multiplying the mixing ratio by $(p/300)^3$, where p is pressure in mb, and then converting the result to molecular column density. The UARS climatology is appended to the temperature profile above 3 mb. The AIRS orbital dataset has the following salient features within a given scene made up of nine FOV's:

- variable surface topography and surface pressure, P_s
- daytime and nighttime conditions
- temperature, $T(p)$, moisture, $q(p)$, ozone, $O3(p)$ from the surface to 0.005 mb
- cloud liquid water profiles, $L(p)$, (only affects microwave)
- multiple level cloudy conditions, within a FOV, with spectrally varying cloud emissivity, $\epsilon_{cld}(\nu)$, and reflectivity, $\rho_{cld}(\nu)$, consistent with atmospheric conditions. The cloud top pressure, emissivity, and reflectivity are spatially varying as well.
- Surface skin temperature, T_s, spectral surface emissivity, $\epsilon(\nu)$ and spectral surface reflectivity, $\rho(\nu)$.
- variable land fraction, with coastlines, islands, lakes, etc.
- orbital simulation with simulated scan lines with variable viewing angle and solar zenith angle.

One simulation simplification has been made. In a real scan line of data, each of the nine MHS and N IR spots that are co-located within a given AMSU-A footprint will have its own zenith angle. Some algorithms (*e.g.*, cloud clearing) need to "correct" the IR radiances to a single zenith angle. The AIRS Science Team developed an algorithm to "correct" the group of nine AIRS spots to the center AIRS footprint (*i.e.*, correct footprint #5 of the nine co-located footprints) for the AIRS instrument; however, we have not developed the coefficients necessary for the IASI or CrIS instruments.

For these reasons, simulation of all IR spots occurs at the zenith angle of the central spot of the IR instrument (spot # 5/9) and simulation of all nine of the MHS spots occurs at the zenith angle of

the MHS's central spot (which is identical to IR instrument in this simulation). The AMSU-A's zenith angle does not equal to the either infrared instrument or MHS. This occurs because AMSU-A steps at 3 $\frac{1}{3}$ degrees while the MHS steps at 1.1 degrees.

5 AIRS/NPOESS Retrieval Algorithm

The retrieval algorithm is similar to the algorithms developed for the AIRS Science Team. The AIRS algorithm is documented within the AIRS algorithm theoretical basis document (*AIRS ATBD* 1997), (*Susskind* 1998), and recent talks given at AIRS Science Team meetings available through the Internet (*SRT* 1997). The current implementation of the AIRS Science Team algorithm consists of three major components: a microwave only retrieval, a first infrared product, and a final infrared product.

The retrieval system used in this study is a research version of the AIRS science team algorithm. This system propagates an ensemble error estimate through the cloud clearing retrieval. The cloud cleared radiance error estimates are propagated through all the statistical and physical retrievals to obtain a case dependent error estimate of all products. The error estimate of the radiances and products are used within the physical retrievals noise covariance matrices for any parameters held constant within that retrieval.

The regression retrieval step uses all the channels. This algorithm and coefficients are provided by the NOAA members of the AIRS Science Team Mitch Goldberg and Yanni Qu. Barnet (*Barnet* 1999) shows that this retrieval is insensitive to apodization, given a well-behaved apodization function. Both Hamming and the Gaussian apodization functions are well-behaved functions.

The final infrared/microwave product uses a physical retrieval with optimized vertical functions similar to the Backus-Gilbert optimization (*Conrath* 1972), (*Backus* 1970), a subset of channels, and information content based on ensemble and case dependent noise estimates, which are propagated through each retrieval.

The first infrared product is used as a first guess for the final retrieval, unless it is rejected. For the AIRS retrieval, a profile is rejected based on the following criteria:

- the fractional cloudiness is greater than 80%.
- the cloud clearing brightness temperature residuals (cloud cleared minus computed from retrieval) are greater than 1.75° K.
- the difference between the bottom two 1-km layer averages of the temperature retrievals exceeds 1.75° K.

We interpret rejection to mean the cloud conditions are too difficult to use cloud contaminated IR radiances. If rejected, then the retrieval of the temperature profile, emissivity, and surface parameters is repeated using the microwave produce and only the AMSU and IR channels insensitive to the clouds.

For the physical retrievals, a subset of channels is used because:

- the noise covariance terms are only estimates and channels with high noise covariance can degrade performance;
- in a given retrieval step, the sensitivity of a channel is determined by the spectral region sampled. Channels are selected which optimize this sensitivity (*Kaplan* 1977). Other channels contribute redundant or negligible information.

During the channel selection process, radiance errors were computed from the retrieved solution for all channels to ensure that the subsetted channels adequately represented the information content of the entire spectrum. The final set of AIRS channels is shown in Figure 3.

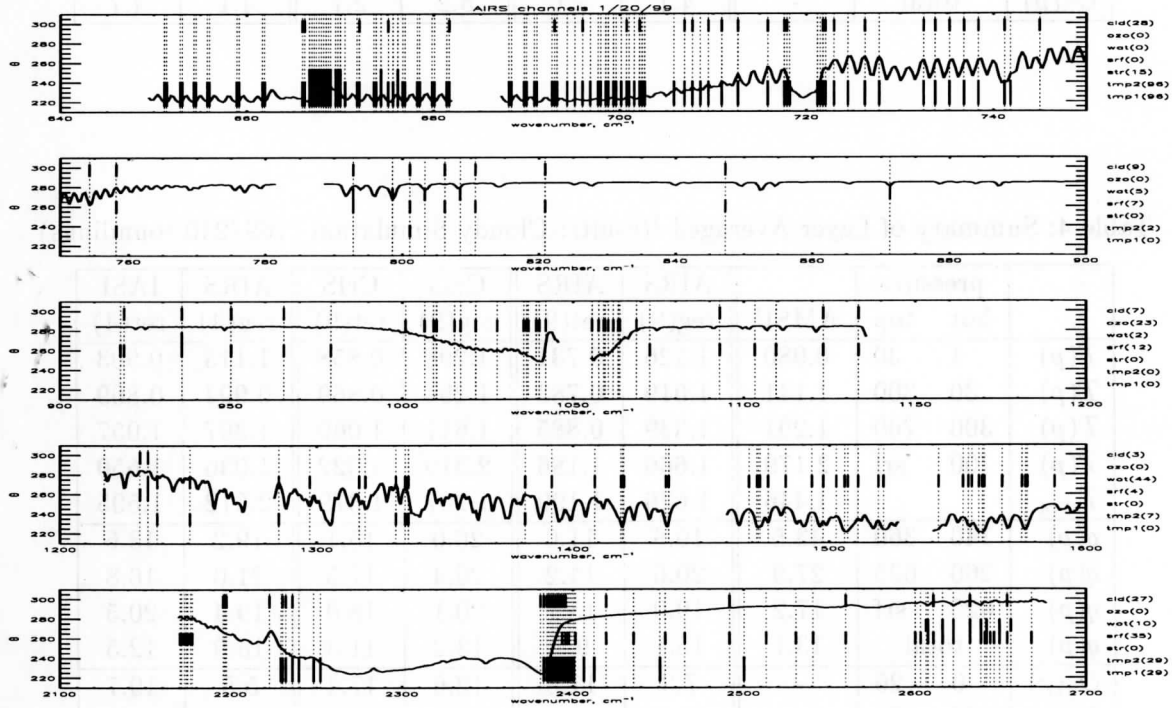

Figure 3: Channels used within AIRS retrieval.

6 Simulation results

Table 3 shows the RMS errors of the "clear" simulation. The average geophysical conditions of the 9 IR footprints within an AMSU footprint comprises the "truth". All simulations were performed for the AIRS Science Team scan lines #2, #4, ..., #16. The "clear" case simulates all FOV's within the

Table 3: Summary of Layer Averaged Results: Clear simulation (229/240 soundings)

	pressure bot	pressure top	AMSU	AIRS reg(9)	AIRS ret(9)	CrIS reg(9)	CrIS ret(9)	AIRS reg(4)	IASI ret(4)
$T(p)$	1	30	1.006	0.676	0.570	0.627	0.552	0.706	0.804
$T(p)$	30	300	1.092	0.713	0.569	0.788	0.603	0.723	0.687
$T(p)$	300	700	1.309	1.008	0.490	0.740	0.500	1.014	0.598
$T(p)$	700	srf	2.151	1.415	0.768	1.545	0.841	1.435	0.916
T_{skin}			4.487	0.492	0.724	0.557	0.813	0.483	0.792
$q(p)$	140	360	63.0	13.6	6.3	14.6	6.2	14.1	8.2
$q(p)$	260	625	26.1	17.0	9.4	16.7	10.9	17.3	10.4
$q(p)$	625	srf	18.2	15.9	12.0	12.1	16.8	16.3	17.2
$q(p)$	total		13.2	14.1	7.7	8.4	14.9	14.4	12.6
$O_3(p)$	0	20	-	4.1	7.7	5.4	7.3	3.9	10.2
$O_3(p)$	20	60	-	14.0	10.1	11.4	9.2	14.0	12.9
$O_3(p)$	60	140	-	12.6	10.8	14.7	9.5	12.7	13.7
$O_3(p)$	140	300	-	7.6	8.4	8.6	8.9	8.1	10.4
$O_3(p)$	300	srf	-	7.0	6.8	9.0	7.9	7.0	11.0
$O_3(p)$	total		-	4.1	2.6	5.2	2.7	4.1	4.7

Table 4: Summary of Layer Averaged Results: Cloudy Simulation (169/240 soundings)

	pressure bot	pressure top	AMSU	AIRS reg(9)	AIRS ret(9)	CrIS reg(9)	CrIS ret(9)	AIRS reg(4)	IASI ret(4)
$T(p)$	1	30	0.980	1.126	0.731	1.298	0.858	1.113	0.903
$T(p)$	30	300	1.141	1.019	0.783	1.294	0.869	0.994	0.869
$T(p)$	300	700	1.291	1.339	0.885	1.611	1.060	1.397	1.057
$T(p)$	700	srf	2.179	1.666	1.186	2.310	1.322	1.936	1.650
T_{skin}			4.446	1.626	1.190	1.267	1.379	2.612	1.595
$q(p)$	140	360	43.5	19.5	11.0	26.0	15.1	19.2	13.6
$q(p)$	260	625	27.9	20.6	14.2	26.4	17.5	21.0	16.8
$q(p)$	625	srf	17.2	19.0	15.7	20.1	18.0	19.4	20.5
$q(p)$	total		13.1	15.1	9.1	13.2	11.3	15.9	12.5
$O_3(p)$	0	20	-	7.3	11.8	12.6	17.4	5.5	19.7
$O_3(p)$	20	60	-	15.9	11.8	23.7	16.6	14.5	18.5
$O_3(p)$	60	140	-	19.1	16.7	30.2	18.8	20.5	18.1
$O_3(p)$	140	300	-	13.4	13.2	26.2	21.0	16.5	17.7
$O_3(p)$	300	srf	-	11.0	13.3	17.6	17.9	11.2	19.3
$O_3(p)$	total		-	6.3	6.9	12.7	8.9	6.3	12.2

AMSU-A footprint as clear (0% cloud fraction and no liquid water) and used 229 of 240 AMSU-A footprints within these scan-lines. The remaining cases were rejected. In all cases, the IR spectra for all footprints within the AMSU-A footprint were averaged.

Table 4 shows the "cloudy" cases. These were simulated with the multi-level clouds and liquid water assigned in the orbital simulation. IR footprints have up to 2 layers of clouds; however, the cloud top pressure and cloud spectral properties vary within the layers and between IR FOV's. We allow the solution of up to 4 cloud formations within the 9-FOV cloud clearing and 3 formations within the 4-FOV cloud clearing.

In Table 3 and Table 4 we show the RMS errors of the results for the AMSU retrieval, AIRS regression and physical retrieval, CrIS regression and physical retrieval, and IASI regression (AIRS 4-FOV) and physical retrieval. The RMS temperature errors were computed in layers (1 km layer from surface to 300 mb, 3 km from 300 to 30 mb, 5 km from 30 to 1 km) and then averaged over the intervals shown in the table. Also shown is surface skin temperature. These tables also show the RMS errors of the water in 2 km layers averaged over the 3 pressure boundaries shown, as well as the total error. For ozone the percent RMS errors are shown for the layers indicated.

Findings for AIRS versus CrIS:

- stratosphere and upper troposphere (primarily from 15 μm region)
  - poorer spectral resolution and sampling of CrIS is not compensated for by lower noise
- lower troposphere (primarily from 4.2 μm region)
  - spectral resolution is not important (lines are not resolved)
  - CrIS noise is much higher causing degraded results
- water vapor (primarily from 6.3 μm region)
  - loss of band coverage (1540-1650 cm^{-1} and 2450-2750 cm^{-1}) degrades performance
  - higher noise in band #2 and #3 degrades performance
- CrIS results degrade more with clouds than do AIRS
  - CrIS noise estimate may be optimistic and requires that other noise sources are not significant (*e.g.*, RTA fitting errors). If CrIS's noise is greater than shown here the results will degrade. Conversely, if better noise is achieved, results should improve.

Findings for AIRS versus IASI (PRELIMINARY):

- stratosphere and upper troposphere (primarily from 15 μm region)
  - spectral resolution is similar
  - IASI's sampling is the same; however, noise in adjacent channels is correlated by 70%.

  - IASI results are worse because IASI's 4-FOV's allows less noise reduction from averaging than does the AIRS 9-FOV's

- lower troposphere (primarily from 4.2 μm region)

  - IASI's improved spectral resolution is not important (lines are still not resolved)
  - IASI noise is much higher
  - IASI sampling is effectively reduced due to noise correlation in adjacent channels
  - significant degradation occurs in cloudy conditions (clouds amplify noise effects)
  - IASI regression first guess needs to be implemented

- water vapor (primarily from 6.3 μm region)

  - higher noise degrades performance; however, we need to test adding more IASI water channels to compensate for the higher noise.

- At present, IASI results degrade more with clouds than do AIRS

References

The AIRS ATBD (currently the Sep. 1997 version) is available through the EOS scientific information Internet site at "http://eospso.gsfc.nasa.gov/". Click on "Scientific Information", "Publications", "Algorithm Theoretical Basis Documents", "AIRS", and then select the level-2 ATBD. The document is in PDF format.

Aumann H.H. and R.J. Pagano, 1994. "Atmospheric infrared sounder on Earth observing system," Optical Engineering **33**, 776-784.

Backus, G. and F. Gilbert, 1970. "Uniqueness in the inversion of inaccurate gross earth data." *Phil. Trans. Roy. Soc. Lond.* **266** p.123-192.

Barnet, C.D., J.M. Blaisdell and J. Susskind, 1999. "An analytical transformation for use in computation of interferometric spectra for remote sensing applications spectra." *IEEE Trans. Geosci. Remote Sens.* In press.

Cayla F., 1993. "IASI infrared interferometer for operations and research." In *High Spectral Resolution Infrared Remote Sensing for Earth's Weather and Climate Studies*, NATO ASI Series, Series I, Vol. 9, edited by A. Chedin, M. Chahine, and N. Scott (Berlin: Springer Verlag), 9-19.

Conrath, B.J., 1972. "Vertical resolution of temperature profiles obtained from remote sensing radiation measurements." *J. Atmos. Sci.* **29** p.1262-1271.

Hannon, S., L.L. Strow, and W.W. McMillan, 1996. "Atmospheric infrared fast transmittance models: a comparison of two approaches." *SPIE* v.2830 **94** 105.

Integrated Programs Office IPO, 1998. The NPOESS CrIS instrument, specified in this paper, is a notional instrument with characteristics published in specification documents by the IPO.

Juang H-M. H., S.Y. Hong, and M. Kanamitsu, 1997. 'The NCEP regional spectral model: an update." *Bulletin Amer. Meteor. Soc.* **78**, p.2125.

Kaplan, L.D., M.T. Chahine, J. Susskind, and J.E. Searl, 1977. "Spectral band passes for a high precision satellite sounder." *Applied Optics* **16** p.322-324.

The Sounder Research Team (SRT) at GSFC homepage is "http://faster.gsfc.nasa.gov/airs.html". Click on "AIRS" and scroll down to "AIRS Science Team Presentations." Select the talks of interest to download. Files are postscript. The recent talks related to the algorithm used within this paper are:

- propagation of error estimates presented at Oct. 31, 1996 meeting
- multiple formation cloud-clearing (w/ 9 AIRS footprints) presented at Oct. 23, 1997 meeting by C. Barnet
- AIRS rejection philosophy and summary of recent results with the AIRS Science Team algorithm presented at the Oct. 23, 1997 meeting by J. Susskind.

Susskind, J., C. Barnet, and J. Blaisdell, 1998. "Determination of atmospheric and surface parameters from simulated AIRS/AMSU sounding data: retrieval and cloud clearing methodology," Advances in Space Research, **21**, p.369-384.

TECHNICAL PROCEEDINGS OF THE TENTH INTERNATIONAL ATOVS STUDY CONFERENCE

Boulder, Colorado

27 January - 2 February 1999

Edited by

J. Le Marshall and J.D. Jasper

Bureau of Meteorology Research Centre, Melbourne, Australia

Published by

Bureau of Meteorology Research Centre

PO Box 1289K, GPO Melbourne, Vic., 3001, Australia

December 1999